

Beam-Pointing Fluctuations in Gain-Guided Amplifiers

S. J. Kuo, D. T. Smithey, and M. G. Raymer

Department of Physics and Chemical Physics Institute, University of Oregon, Eugene, Oregon 97403

(Received 4 February 1991)

We report a measurement of the quantum-mechanical beam-pointing fluctuations in the output of a gain-guided, single-pass amplifier using stimulated Raman scattering. The experimental result is in reasonable agreement with a theoretical model that incorporates the effects of excess spontaneous noise associated with the transverse modes of a gain-guided amplifier.

PACS numbers: 42.50.-p, 42.55.Vc, 42.60.Jf, 42.65.Dr

Macroscopic quantum-mechanical fluctuations of light have been observed in a number of single-pass stimulated processes, such as stimulated Raman scattering (SRS),¹ superfluorescence,² amplified spontaneous emission,³ and the transient buildup of a pulsed laser.⁴ These processes involve light initiated from spontaneous noise and amplified to a macroscopic level in a gain medium without a cavity. The fluctuations can occur in the spatial, temporal, or spectral domain. In addition, laser spectra broader than that expected from standard laser theory have been predicted⁵ and observed⁶ for gain-guided lasers. This has been explained in terms of so-called excess spontaneous noise, which arises in systems governed by wave equations or boundary conditions having non-Hermitian properties. These include gain-guided amplifiers,^{5,7} unstable resonators,⁸ and resonators with strong output couplings.⁹ Since Raman generators are gain-guided amplifiers, one might expect that their macroscopic fluctuations would be affected by excess noise. This paper reports beam-pointing fluctuations in Raman generation and compares the experimental results with a theoretical model that incorporates the excess spontaneous noise effect.

Ordinary spontaneous noise refers to the fact that there is one extra photon emitted per mode due to quantum-mechanical uncertainty for systems governed by Hermitian wave equations. For non-Hermitian systems, there is more than one extra photon per mode emitted, and this is characterized by the excess-noise factor^{5,7} which is always greater than unity. This is because the mode functions in Hermitian systems are orthogonal, while the mode functions in non-Hermitian systems are not orthogonal. As a result, the mode amplitudes are independent in the former case, and are correlated in the latter case. It was pointed out by Haus and Kawakami that the excess-noise factor does not lead to an increased total spontaneous emission rate, which would violate thermodynamics.⁷ It is also shown that for loss-guided systems or gain-guided systems, for which gain discrimination between modes is not significant, the spontaneous emission rate per mode projected onto an orthogonal basis is not enhanced. In high-gain amplifiers, where gain discrimination is significant, excess noise can pro-

duce an observable effect.

Recently, the nonorthogonal mode-expansion approach has been applied to single-pass x-ray lasers to predict their transverse spatial coherence properties.¹⁰ The x-ray laser involves photons initiated from spontaneous emission and amplified in an open-ended gain-guided medium, in a fashion similar to that in a Raman generator. Since nonuniform, high gain is usually employed in these processes, gain discrimination between different nonorthogonal modes is expected to be significant. In analogy to the excess-noise effect observed in the longitudinal-mode spectra of semiconductor lasers,⁶ the effects due to the excess-noise factor associated with the transverse nonorthogonal modes in a gain-guided amplifier should be observable if one measures, for example, the fluctuations in the angular distribution of the amplifier output.

To guarantee that the angular distribution of the output of a pulsed Raman generator does not change during a single pulse due to collisional dephasing, a transient condition must be met, i.e., the pump-pulse duration must be short compared to the inverse Raman linewidth of the medium. The spatial distribution of the output from such a Raman generator has been shown to exhibit macroscopic fluctuations in the form of a randomly speckled distribution when the Fresnel number F , defined to be the cross-sectional area of the pump beam divided by the Stokes wavelength and interaction length, is large.¹¹ When F is small, the beam is always near Gaussian, but its direction of propagation fluctuates from shot to shot.¹² We refer to this effect as beam-pointing fluctuations. The connection between the macroscopic spatial fluctuations and quantum-mechanical uncertainty can be understood in terms of a mode expansion of the Stokes field; the Raman generator output is a superposition of waves that are initiated from quantum noise, and subsequently amplified to a macroscopic level. Thus a study of the spatial fluctuations of Stokes light can provide information on the spatial coherence properties of a noise-initiated, single-pass, high-gain amplifier.

It is important to note that beam-pointing fluctuations in stimulated Raman generation were first treated in a calculation by Walmsley,¹³ in which the gain was as-

sumed to be spatially uniform, and no excess-noise effects were present. Another example of beam-pointing fluctuations in the absence of excess-noise effects was observed in a stable-cavity krypton-ion laser by Levenson, Richardson, and Perlmutter.¹⁴ In a gain-guided Raman generator, the beam-pointing fluctuations are not *caused* by the excess noise; rather, they are *influenced* by it, and a quantitative theory of beam-pointing fluctuations must account for this.

We first consider a linearly polarized Stokes field envelope $E_S(\mathbf{r})$ satisfying the paraxial wave equation in the unsaturated gain regime¹⁰

$$\left[\nabla_{\perp}^2 + 2ik_S \frac{\partial}{\partial z} - ik_S g(\boldsymbol{\rho}) \right] E_S(\mathbf{r}) = -4\pi P_s(\mathbf{r}), \quad (1)$$

where $g(\boldsymbol{\rho})$ is the radially dependent gain profile, k_S is the Stokes wave number, and $P_s(\mathbf{r})$ is the spontaneous noise term that has a quantum-mechanical origin, and is treated as a δ -correlated, Gaussian random variable.¹⁵ The Stokes field can be expressed by the mode expansion

$$E_S(\mathbf{r}) = \sum_n b_n(z) u_n(\boldsymbol{\rho}). \quad (2)$$

Because the Stokes field is a Gaussian random process, the b_n 's are correlated, complex, Gaussian random variables. The mode functions $u_n(\boldsymbol{\rho})$ are taken to be the eigenfunctions of the homogeneous transverse part of Eq.

(1), and thus satisfy a non-Hermitian equation

$$[\nabla_{\perp}^2 - ik_S g(\boldsymbol{\rho})] u_n(\boldsymbol{\rho}) = -i2k_S q_n u_n(\boldsymbol{\rho}), \quad (3)$$

where q_n is the complex eigenvalue. The mode functions are not orthogonal,

$$B_{mn} = \int d^2\rho u_m^*(\boldsymbol{\rho}) u_n(\boldsymbol{\rho}) \neq \delta_{mn}, \quad (4a)$$

but are biorthogonal,

$$\int d^2\rho u_m(\boldsymbol{\rho}) u_n(\boldsymbol{\rho}) = \delta_{mn}. \quad (4b)$$

The term B_{mn} , which occurs in the expression of power density per mode for mode n , is always greater than unity, and is called the excess-spontaneous-noise factor. The mode amplitudes are correlated according to

$$C_{mn} \equiv \langle b_m^*(z) b_n(z) \rangle = AB_{mn} \{ \exp[(q_m^* + q_n)z] - 1 \}, \quad (5)$$

where A is a constant. This means that noise can feed into the dominant mode from all other modes and vice versa.⁷ Also there is gain discrimination between modes, due to the overlap of each mode with the gain profile. Note that the subscript n in Eqs. (2)–(5) is a shorthand notation for a set of two indices $n \equiv (j, j')$ corresponding to $u_n(\boldsymbol{\rho}) \equiv \phi_j(x) \phi_{j'}(y)$ and $q_n \equiv q_{jj'} = \lambda_j + \lambda_{j'}$, where λ_j is an eigenvalue associated with the one-dimensional mode function $\phi_j(x)$. A similar convention is used for the subscript m in Eqs. (2)–(5).

To characterize the beam-pointing fluctuations, we use the mean transverse \mathbf{k} vector, defined as

$$K_x = \frac{-i \int dt \int dx E_S^*(x, y=0, z=L, t) (\partial/\partial x) E_S(x, y=0, z=L, t)}{\int dt \int dx E_S^*(x, y=0, z=L, t) E_S(x, y=0, z=L, t)}, \quad (6)$$

where the Stokes field is evaluated at the output face of the medium with the y coordinate chosen to be at the center of the Stokes beam ($y=0$). An alternative definition for the mean transverse \mathbf{k} vector of the whole beam can be defined by integrating over y in both the numerator and the denominator in Eq. (6).¹³ The sliced-beam definition of Eq. (6) will be used to compare with experiment in this Letter. The numerator in Eq. (6) represents the mean value of the transverse component of the Poynting vector for a single realization, and the normalization ensures that individual realizations carry equal statistical weight. The far-field propagation angle can be expressed as $K_x \lambda / 2\pi$, where λ is the Stokes wavelength. The probability distribution of finding the mean \mathbf{k} vector having a value K_x' is

$$\begin{aligned} P(K_x') &= \langle \delta^2(K_x - K_x') \rangle \\ &= \frac{1}{2\pi} \int d^2\xi \exp(-iK_x' \xi) \langle \exp(iK_x \xi) \rangle. \end{aligned} \quad (7)$$

Substituting the mode expansion for a transient Stokes field into Eq. (6), the mean transverse \mathbf{k} vector can be expressed as

$$K_x = \frac{\sum_m \sum_n b_m^* b_n U_{mn}}{\sum_m \sum_n b_m^* b_n B_{mn}}, \quad (8)$$

where

$$U_{mn} = -i \int dx u_m^*(x, 0) \frac{\partial}{\partial x} u_n(x, 0).$$

The probability distribution $P(K_x')$ can then be expressed rigorously in terms of the matrix elements of C_{mn} , B_{mn} , and U_{mn} .^{13,16}

For a Raman generator of length L pumped by a laser pulse with a Gaussian spatial profile of radius a , the transverse gain profile can be approximated by $g(\boldsymbol{\rho}) = g_0(1 - \rho^2/a^2)$, where g_0 is the plane-wave gain coefficient. The quadratic approximation treats the outer portion of the medium as an absorbing one. Since amplification of spatial modes occurs predominantly inside the region where gain is positive, the absorbing portion of the profile has little effect. The solutions for Eq. (3) are two-dimensional Gauss-Hermite functions with complex argument $(-iF_e)^{1/4} x/a$ and $(-iF_e)^{1/4} y/a$, where $F_e = Gk_S a^2/L$ is an effective Fresnel number, and $G = g_0 L$. The eigenvalue is given by

$$g_{jj'} = \frac{g_0}{2} \left[\frac{2j+1}{(-iF_e)^{1/2}} + \frac{2j'+1}{(-iF_e)^{1/2}} + 1 \right]. \quad (9)$$

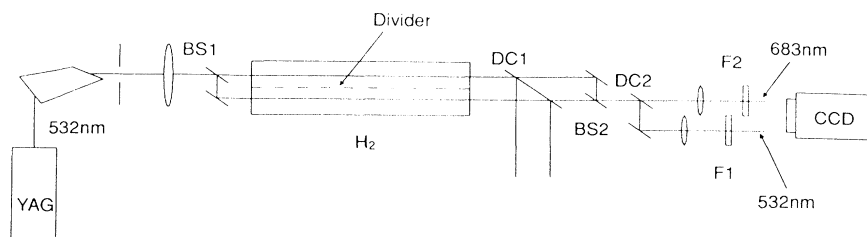


FIG. 1. Apparatus for generating two independent Stokes beams which are combined to produce an interference pattern. Interference patterns of Stokes light and pump light are recorded on a CCD camera.

To describe the propagation of the Stokes field in the transient regime, it can be shown that the steady-state plane-wave gain coefficient g_0 should be replaced by $g_0\tau_S\Gamma/2$ in Eq. (1),¹⁶ where Γ is the Raman linewidth and τ_S is the Stokes pulse duration.¹⁷ This accounts for the well-known lower amplification of Stokes field in the transient regime and allows treatment of the transverse spatial properties in detail.

In our experiment, we use an interferometric method to measure the mean transverse \mathbf{k} vector. Consider two plane waves crossing at a small angle; the period of the interference pattern formed in the spatial intensity distribution is equal to the inverse of the difference of the transverse components between the two wave vectors. The periodicity of such an interference pattern is independent of the relative amplitudes of the individual fields. Thus measuring the periodicity of the interference pattern formed by two independently generated Stokes fields approximately gives the relative mean transverse \mathbf{k} vector, $K_{x2} - K_{x1}$. The standard deviation K_x of a single beam can be obtained from the standard deviation of $K_{x2} - K_{x1}$ by $\Delta K_x = \Delta(K_{x2} - K_{x1})/\sqrt{2}$. This equivalence is approximate because the Stokes fields are not truly plane waves. The interferometric setup has the advantage that any directional fluctuations of the pump pulse will not affect the interference pattern of the Stokes field.

The experimental setup is shown in Fig. 1. A Nd-doped yttrium-aluminum-garnet laser is frequency doubled to produce linearly polarized pulses at 532 nm with duration $\tau_L = 300$ ps at full width at half maximum (FWHM). The output pulse is spectrally filtered to remove extraneous light at the Stokes frequency which could act as a seed for SRS generation. The pump beam is split into two equal-intensity beams and sent inside a Raman cell 1 m long containing hydrogen gas at 40 atm. The collisional linewidth Γ of the $Q(1)$ transition in H_2 is 6.5×10^9 rad/s at this pressure.¹⁸ The two parallel pump beams are 1 cm apart, and a metal divider is inserted inside the cell to eliminate cross talk between the two parallel beams. The diameter $2a_{1/2}$ at FWHM of the pump pulse is varied from 0.98 to 1.94 mm, corresponding to Fresnel number $F = \pi a_{1/2}^2/\lambda L$ between 1.1 and 4.3. The longitudinal variation of the pump beam radius is 12% for the smallest Fresnel number, and 8%

for the largest Fresnel number. This justifies the approximation that the gain profile does not change longitudinally. The Raman gain coefficient g_0 is estimated from laser intensity measurements to be between 0.34 and 0.38 cm^{-1} .¹⁸ The condition $\Gamma\tau_L < g_0L$ is thus satisfied, and the Stokes-photon conversion efficiency is kept below 10^{-4} , ensuring that the SRS is in the transient, unsaturated regime. The Stokes pulse duration τ_S is calculated to be 180 ps, in agreement with streak-camera observations. A dichroic mirror DC1 rejects 99% of the pump light in both beams. A second beam splitter BS2 is used to combine the two transmitted beams at a small angle of several milliradians. The recombined beam, which contains pump and Stokes light, is spectrally separated by a second dichroic mirror DC2 and filters F1 and F2. The pump and Stokes fields near the output face of the cell are imaged onto different regions of a charge-coupled-device (CCD) camera. This allows the recording of interference patterns formed by the two Stokes beams, as well as those formed by two pump beams. We recorded a narrow slice at $y=0$ of each interference pattern. To ensure the Stokes gain is nearly reproducible, the laser pulse energy is recorded for each shot, and data are collected only if the energy is within $\pm 1.5\%$ of the average. The number of samples in each data set corresponding to a particular Fresnel number is about 300 or more.

Figure 2 shows two recorded interference patterns for Fresnel number $F=3.6$, demonstrating different periodicities. To obtain the relative mean transverse \mathbf{k} vector ($K_{x2} - K_{x1}$) from a quasiperiodic intensity distribution as shown in Fig. 2, we calculate the Fourier transform of

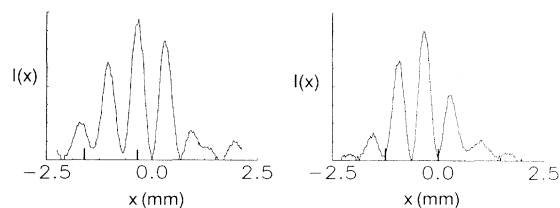


FIG. 2. Two examples of single-shot interference patterns of Stokes light. Different periodicities are seen, indicating fluctuations of the beam-pointing angle (transverse \mathbf{k} vector).

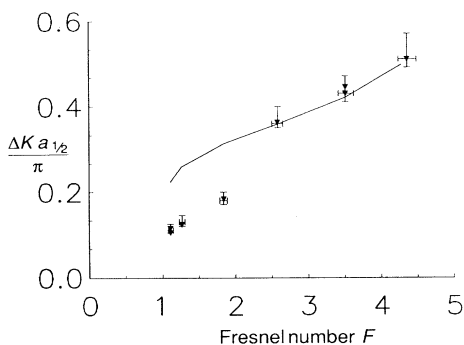


FIG. 3. The triangles are the measured standard deviation of the mean transverse \mathbf{k} vector normalized to $\pi/a_{1/2}$. The ordinate can be interpreted as the standard deviation of the beam-pointing angle divided by its diffraction-limited angle. The error bars are lower-bound estimates of variations due to digitization, pump fluctuations, and statistical errors. The solid curve shows predictions from the biorthogonal-mode model that incorporates excess-noise effects.

the intensity distribution, which contains a dc peak and symmetrically located peaks at the spatial modulation frequency. To obtain the relative mean transverse \mathbf{k} vector for a single shot, we calculate the average of the square modulus of the positive-frequency peak.

Figure 3 shows the standard deviation ΔK_x plotted versus the Fresnel number. The ordinate is normalized to $\pi/a_{1/2}$. Figure 3 also shows the theoretical predictions for the beam-pointing standard deviation using the biorthogonal-mode method presented above. The increase in ΔK_x is expected; the number of spatial modes increases when the Fresnel number becomes larger, allowing a greater number of spatial modes to contribute more to the distortion of the wave front of the field. While the trend of the data and theory (with no free parameters) agrees, there is absolute agreement only at the large Fresnel numbers. The reason for the systematic disagreement at low F is unknown.

In conclusion, the beam-pointing fluctuation provides information on the transverse-mode structure of light generated from a single-pass, gain-guided amplifier, on the gain discrimination between the spatial modes, and on macroscopic spatial fluctuations caused by quantum-mechanical uncertainty. The observed beam-pointing fluctuation of light from transient SRS increases with increasing Fresnel number, and at $F=5$ the fluctuation is about 50% of the diffraction-limited angle defined by the

pump beam aperture. This fluctuation is about 1000 times greater than that observed in a standard gas laser, where the modes are defined by the stable cavity and are orthogonal.¹⁴ In gain-guided amplifiers, such as SRS, the modes defined by the spatial gain distribution are not orthogonal. The experimental result agrees reasonably well with a theoretical model (with no free parameters) that incorporates the excess-spontaneous-noise effect associated with the transverse modes of a gain-guided amplifier. The increase in beam-pointing fluctuations with increasing Fresnel number could have significant implications in cavityless x-ray lasers, which have dynamics similar to SRS, but usually have much larger Fresnel number because of the shorter wavelength.

We wish to thank Ian Walmsley for helpful discussions. This research was supported by the U.S. Army Research Office.

¹I. A. Walmsley and M. G. Raymer, Phys. Rev. Lett. **50**, 962 (1983).

²H. M. Gibbs, Q. H. F. Vrehen, and H. M. S. Hickspeer, Phys. Rev. Lett. **39**, 547 (1977).

³S. P. Kravis and L. Allen, Opt. Commun. **23**, 289 (1977).

⁴F. T. Arecchi, V. Degiorgio, and B. Querzola, Phys. Rev. Lett. **19**, 1168 (1967).

⁵K. Petermann, IEEE J. Quantum Electron. **15**, 566 (1979).

⁶W. Streifer, D. R. Serfres, and R. D. Burnham, Appl. Phys. Lett. **40**, 305 (1982).

⁷H. Haus and S. Kawakami, IEEE J. Quantum Electron. **21**, 63 (1985).

⁸A. E. Siegman, Phys. Rev. A **39**, 1253 (1989).

⁹W. A. Hamel and J. P. Woerdman, Phys. Rev. A **40**, 2785 (1989); Phys. Rev. Lett. **64**, 1506 (1990).

¹⁰R. A. London, M. Strauss, and M. D. Rosen, Phys. Rev. Lett. **65**, 563 (1991).

¹¹M. A. Henesian, C. D. Swift, and J. R. Murray, Opt. Lett. **10**, 565 (1985).

¹²S. J. Kuo, C. Radzewicz, and M. G. Raymer, in *Proceedings of OSA Annual Meeting, Rochester, New York, 1987* (Optical Society of America, Washington, DC, 1987).

¹³I. A. Walmsley, J. Opt. Soc. Am. B **8**, 805 (1991).

¹⁴M. D. Levenson, W. H. Richardson, and S. H. Perlmutter, Opt. Lett. **14**, 779 (1989).

¹⁵F. Haake and R. J. Glauber, Phys. Lett. **68A**, 29 (1979).

¹⁶S. J. Kuo, Ph.D. thesis, University of Rochester, 1991 (unpublished).

¹⁷M. G. Raymer, I. A. Walmsley, J. Mostowski, and B. Sobolewska, Phys. Rev. A **32**, 332 (1985).

¹⁸W. K. Bischel and M. T. Dyer, J. Opt. Soc. Am. B **3**, 677 (1986).